The influence of mass diffusion on the photothermal signals detected via the mirage effect. I. Theory

1995 J. Phys.: Condens. Matter 7 9385

(http://iopscience.iop.org/0953-8984/7/49/005)

J. Phys.: Condens. Matter 7 (1995) 9385–9399. Printed in the UK

The influence of mass diffusion on the photothermal signals detected via the mirage effect: I. Theory

M Z Silva†§, F Lepoutre† and P Korpiun‡

† Laboratoire d'Optique Physique, ESPCI, 10 rue Vauquelin, 75005 Paris, France
‡ Physik-Department E13, Technische Universität München, 8046 Garching, Germany

Received 19 June 1995

Abstract. This paper presents a theoretical study of the influence of mass diffusion on the photothermal signals detected by the mirage effect. A model is developed for the mirage effect when physical adsorption occurs on a non-porous sample under conditions close to the normal temperature and pressure. It shows that the mass diffusion contribution to the mirage deflection, due to the induced periodic adsorption/desorption of vapour molecules at the solid sample surface, may become more important than the thermal contribution due to the temperature gradient. The model also predicts that the mirage deflection can be used to experimentally determine the mass diffusion coefficient of a binary gas mixture The limits of validity of this simple one-dimensional theory are discussed and an analysis of the influence of the experimental parameters is presented. An interesting result of this discussion is that the phase of the mirage signal is remarkably sensitive to the adsorbed film growth when the magnitudes of the thermal and the mass diffusion contributions are similar.

1. Introduction

A few experiments [1–6] have demonstrated that photothermal methods are sensitive to adsorption of liquids on solid surfaces. The basic idea is the monitoring of a periodic desorption via absorption of a modulated light flux at the surface. The detection can be achieved either by detecting the pressure variations produced by the periodic adsorption and desorption (photoacoustic) with a microphone or by measuring the deflection of a light beam skimming the surface with a position sensor (e.g. a quadrant cell). This method (the mirage effect method) is a rather well established technique for performing optical absorption measurements or thermal characterizations. Principally, the method consists in heating the specimen with a modulated light beam and detecting the periodic surface temperature by measuring the deflection of a second beam skimming the surface.

The first quantitative explanations of the detection of adsorption by photothermal techniques were given by Korpiun [2] for the photoacoustic effect and were generalized to the mirage effect in further papers [4, 5]. In this work [4, 6], the mirage effect was shown to be directly sensitive to the gradient of the adsorbable molecules in the gas close to the surface.

Here, we present a theoretical study of the influence of mass diffusion on the photothermal signals detected by the mirage effect. First, in section two, we develop the theoretical model and we establish an expression for the mirage deflection when an

§ Present address: Departamento de Fisica, Universidad do Minho, 4700 Braga, Portugal.

0953-8984/95/499385+15$19.50

adsorbed film is formed over the sample surface. In sections three and four, we analyse respectively the thermal and the mass diffusion contributions to the mirage deflection and we discuss the influence of each one of the experimental parameters when one of these contributions dominates. In section five we present the results of simulations made using the theoretical model and, in the last section, we discuss the conditions that provide the maximum sensitivity of the mirage deflection to the adsorption process.

2. Mirage deflection

2.1. Hypotheses

Let us consider a closed cell containing a solid sample S at temperature T and a mixture of two gases A and B with C_A and C_B the respective numbers of moles per unit volume (mole concentration). B can be condensed at a temperature close to T while A cannot be condensed under the experimental conditions used.

We assume that a thin film of adsorbed B molecules is formed at the surface of S which receives a modulated flux of light (a pump beam; see figure 1). We also assume that the film is transparent and that all of the pump beam is absorbed at the sample surface. This film is partially vaporized during the half-period of illumination of the sample.

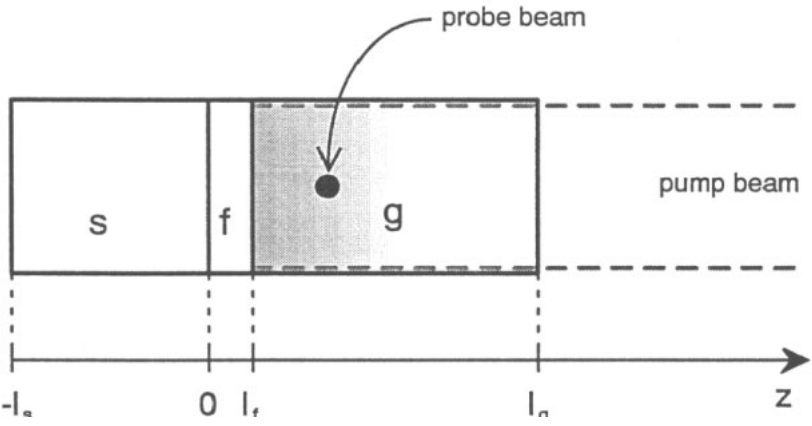

Figure 1. A schematic representation of the mirage detection. s: sample; f: film; g: gas mixture. The window is at $z = l_g$.

A second beam (the probe beam) skims the sample at a distance z (figure 1) and is deflected by the gradient of the logarithm of the gas refractive index n, itself produced by both the temperature gradient $\partial T/\partial z$ and the molecular gradients $\partial C_A/\partial z$, $\partial C_B/\partial z$:

$$\Phi_n = \frac{1}{n}\frac{\partial n}{\partial T}\frac{\partial T}{\partial z} + \frac{1}{n}\frac{\partial n}{\partial C_A}\frac{\partial C_A}{\partial z} + \frac{1}{n}\frac{\partial n}{\partial C_B}\frac{\partial C_B}{\partial z}. \tag{1}$$

The first term of expression (1) is the thermal contribution proportional to the derivative of n versus the temperature T. The second and the third ones are the contributions of the molecular gradients, they are proportional to the derivatives of n versus C_A and C_B.

One can easily show [7] that the refractive index of a binary mixture is given by

$$n - 1 = \frac{RT_0}{P_0}\left[C_A\left(n_A^0 - 1\right) + C_B\left(n_B^0 - 1\right)\right] \tag{2}$$

where R is the ideal-gas constant and the index zero denotes quantities evaluated at NTP conditions (pressure P_0 and temperature T_0). Since the sound wavelength in the cell is much larger than the cell length, one can assume that the total number of moles per unit volume, C, is independent of the position z:

$$\frac{\partial C}{\partial z} = \frac{\partial C_A}{\partial z} + \frac{\partial C_B}{\partial z} = 0. \tag{3}$$

With the help of relations (2) and (3), the mirage deflection can be written as

$$\Phi_n = -\frac{1}{n}\frac{RT_0}{P_0}\left\{\left[C_A\left(n_A^0 - 1\right) + C_B\left(n_B^0 - 1\right)\right]\frac{1}{T}\frac{\partial T}{\partial z} - \left(n_B^0 - n_A^0\right)\frac{\partial C_B}{\partial z}\right\}. \tag{4}$$

In this expression Φ_n depends on the position z through the two gradients $\partial T/\partial z$, $\partial C_B/\partial z$ which are evaluated in the next section.

2.2. Temperature and concentration gradients

The media presented of figure 1 are characterized by their thicknesses, thermal conductivities k_i, and diffusivities α_i. We assume that the ligth flux contains a periodic part which is written as Q:

$$Q = Q_0 e^{i\omega t} \tag{5}$$

which is absorbed totally at the surface of an optically opaque sample and completely converted to heat.

The periodic temperatures (temperature waves) in the three media are solutions of heat diffusion equations with the classical boundary conditions, continuity of temperatures and fluxes, modified by the heat of adsorption. For these calculations, we considered that the sound pressure which is generated in the cell does not affect the periodic temperature. This is not rigorous but it has been shown [8] that the 'acoustic' temperature is almost uniform in the gas in a cell that is small compared with the sound wavelength. Since the mirage detection is only sensitive to the temperature gradient (equation (4)), the 'acoustic' temperature can be neglected with a very high degree of precision.

If adsorption takes place at the film–gas interface ($z = l_f$) and optical absorption at the substrate–film interface ($z = 0$), the temperature waves in the gas, the film and the substrate are respectively

$$\tilde{T}_g = T_{g_0} e^{-(1+i)(z-l_f)/\mu_g + i\omega t} \qquad (z > l_f) \tag{6}$$

$$\tilde{T}_f = T_f^+ e^{(1+i)z/\mu_f + i\omega t} + T_f^- e^{-(1+i)z/\mu_f + i\omega t} \qquad (0 < z < l_f) \tag{7}$$

$$\tilde{T}_s = T_{s_0} e^{(1+i)z/\mu_s + i\omega t} \qquad (z < 0) \tag{8}$$

where μ_i is the thermal diffusion length in medium i:

$$\mu_i = \sqrt{\frac{\alpha_i}{\pi f}}. \tag{9}$$

$\alpha_i = k_i/(\rho_i c_{pi})$ is the thermal diffusivity (with the thermal conductivity k_i, the density ρ_i and the isobaric specific heat capacity c_{pi} of medium i). Writing equations (6) and (8), we suppose that the gas and the solid sample are thermally thick, i.e. $l_g \gg \mu_g$ and $l_s \gg \mu_s$ and that the radiative and convective losses are negligible.

The periodic temperature at $z = l_f$, with amplitude T_{g_0}, is coupled to the molecular flow of molecules B at the interface $z = l_f$ by the heat needed to separate a mole B from the surface. This coupling term will be calculated below.

The next problem is the calculation of the spatial distribution of the condensable molecules B. We write:

(i) the mole fraction X of condensable molecules B as

$$X = \frac{C_B}{C_A + C_B} = \bar{X} + \chi e^{i\omega t} \tag{10}$$

where $\bar{X}$ and χ are the DC and the AC parts respectively of X; and

(ii) the total number of moles per unit volume (molar concentration) $C = C_A + C_B$ as

$$C = \bar{C} + c\, e^{i\omega t} \tag{11}$$

where $\bar{C}$ and c are the DC and AC parts respectively of C and $|c| \ll \bar{C}$. $\bar{C}$ and c are independent of z [5].

The diffusive molecular flows of A or B are given by the Fick law [9]:

$$j_{A,B} = -D\frac{\partial C_{A,B}}{\partial z} + C_{A,B}V \tag{12}$$

where D is the mutual diffusion coefficient and V is the molar average velocity (which is sometimes called the convective velocity though this notation can lead to confusion with the thermal convective velocity which is not taken into account in equation (12)). If the sinusoidal excitation vanishes, an equilibrium is reached, so $\partial C_{A,B}/\partial_z = 0$ and $j_{A,B} = 0$. Thus, from its definition, V only exists when the periodic excitation is applied, which means that V is only an AC term:

$$V = v(z)\, e^{i\omega t}. \tag{13}$$

From (12) this velocity can easily be related to the total molar diffusive flow. Neglecting all terms non-linear in the small quantities c and v [5], we have

$$j_A + j_B = v(z)\,\bar{C}\, e^{i\omega t}. \tag{14}$$

The derivative versus z of equation (12) applied to molecules B using equations (10), (11) and (13) is, in the linear approximation, equal to

$$\frac{\partial j_B}{\partial z} = \bar{C}\left[-D\frac{\partial^2 \chi}{\partial z^2} + \bar{X}\frac{\partial v}{\partial z}\right] e^{i\omega t} \tag{15}$$

which leads, with the equation of continuity, to

$$\bar{C}\left[-D\frac{\partial^2 \chi}{\partial z^2} + \bar{X}\frac{\partial v}{\partial z}\right] = -i\omega\left[\chi\bar{C} + \bar{X}c\right] \tag{16}$$

if all non-linear terms are neglected.

The conservation of the total number of moles per unit volume in the same approximation

$$\frac{\partial (j_A + j_B)}{\partial z} = -i\omega c = \bar{C}\frac{\partial v}{\partial z} \tag{17}$$

allows us to simplify (16):

$$D\frac{\partial^2 \chi}{\partial z^2} = i\omega\chi \tag{18}$$

which means, as mentioned by Korpiun *et al* [5], that the concentration χ of molecules B is determined by a diffusion equation, the solution of which gives the concentration wave:

$$\chi\bar{C} = \chi_0\bar{C}\, e^{-(1+i)(z-l_f)/\mu_D} \tag{19}$$

where

$$\mu_D = \sqrt{\frac{D}{\pi f}} \tag{20}$$

is the mass diffusion length in the gas.

The molar concentration C_B of the component B is given by (from equations (10) and (11), and neglecting the non-linear terms)

$$C_B = \bar{X}\bar{C} + c_B\,e^{i\omega t} \tag{21}$$

where c_B, the periodic variation of the number of moles B, is equal to

$$c_B = \chi\bar{C} + c\bar{X} \tag{22}$$

so its spatial derivative $\partial c_B/\partial z$ is equal to

$$\frac{\partial c_B}{\partial z} = \bar{C}\frac{\partial \chi}{\partial z} = -\chi_0\bar{C}\,\frac{1+i}{\mu_D}\,e^{-(1+i)(z-l_f)/\mu_D}. \tag{23}$$

The number of moles of vapour adsorbed on one square metre, the uptake Y (mol m^{-2}), depends on temperature T and vapour pressure P_B or, if P is constant, on T and the mole fraction $X = P_B/P$. Here, $P = P_A + P_B$ is the total pressure at T.

In the adsorption/desorption phenomena an adsorbed phase is involved whose complete characterization implies the use of three independent parameters, for instance: pressure, temperature and number of adsorbed moles Y per unit surface area.

As a result, for instance, on a $P = f(T)$ representation we can draw an infinity of curves representing the required conditions for thermodynamical equilibrium between the gaseous and the adsorbed states, each one of these curves corresponding to a different amount of adsorbed matter; these are termed isosteres.

Thus, the flux of vapour at the interface $z = l_f$

$$j_B\,(l_f, t) = -\frac{\partial Y}{\partial t} \tag{24}$$

becomes

$$j_B\,(l_f, t) = -\left(\frac{\partial Y}{\partial T}\right)_{P_B}\left(\frac{\partial \tilde{T}_g}{\partial t}\right)_{z=l_f} - \left(\frac{\partial Y}{\partial P_B}\right)_T R\bar{T}\left[\frac{\partial}{\partial t}(XC)\right]_{z=l_f} \tag{25}$$

where $\bar{T}$ is the DC part of T ($\bar{T} \gg |\tilde{T}_g|$).

The first term in equation (25) indicates that the flux of vapour released from the substrate due to temperature variation increases proportionally to its amplitude T_{g_0}, equation (6), since $\partial(Y/\partial T)_{P_B} \leqslant 0$. The second term describes the reduction of the desorption by the increasing vapour concentration controlled by diffusion and convection.

The coefficients $(\partial Y/\partial T)_{P_B} \equiv Y_T$ and $(\partial Y/\partial P_B)_T \equiv Y_P$ determine the distance between the isosteres. If one assumes the Clausius–Clapeyron relation to be valid, the ratio of the coefficients is related by the equation

$$\frac{Y_T}{Y_P} = -\frac{P_B}{RT^2}L \tag{26}$$

to the isosteric heat of sorption, L, of one mole of B.

The coefficient Y_P is equal to the slope of the adsorption isotherm. This quantity is the one that is commonly measured in conventional adsorption experiments [10, 11].

Using equation (6) for $\tilde{T}_g$, equation (11) for C, and equations (10) and (19) for X, the flux of vapour, $j_B(l_f, t)$ (equations (24) and (25)), becomes, in the linear approximation,

$$j_B\left(l_f, t\right) = -\mathrm{i}\omega\left[Y_T T_{g_0} + R\bar{T}Y_P\left(\chi_0\bar{C} + c\bar{X}\right)\right]\mathrm{e}^{\mathrm{i}\omega t} \tag{27}$$

or with equation (26)

$$j_B\left(l_f, t\right) = -\mathrm{i}\omega R Y_P\left[T_{g_0}\frac{P_B L}{R^2T^2} + \bar{T}\left(\chi_0\bar{C} + c\bar{X}\right)\right]\mathrm{e}^{\mathrm{i}\omega t}. \tag{28}$$

We obtain a second relation for the flux of vapour from equation (12) using the condition $j_A = 0$ at the boundary of the adsorbate to the gas $z = l_f$ and equation (3):

$$j_B\left(l_f, t\right) = (1+\mathrm{i})\frac{\chi\bar{C}D}{\mu_D\left(1-\bar{X}\right)}\mathrm{e}^{\mathrm{i}\omega t}. \tag{29}$$

In order to further eliminate the concentration variation c from equation (28) we need another expression relating this quantity to the variation $\chi\bar{C}$ in concentration. This relation is deduced from the condition that the flux $j_B(l_f, t)$ crossing the boundary of area S between the adsorbate and the gas varies the total concentration in the volume Sl_g of the gas by an amount that is given by

$$\int_{Sl_g}\frac{\partial j_B(z,t)}{\partial z}\,\mathrm{d}V = \int_{S_t} j_B(z,t)\,\mathrm{d}S = \int_{Sl_g}\frac{\partial C}{\partial t}\,\mathrm{d}V \tag{30}$$

where S_t is the total surface area of the gas volume Sl_g. Since $j_B(z,t) \neq 0$ only holds for the area S at $z = l_f$, and since we are dealing with a monodimensional problem, equation (30) becomes, with $j_B(l_f, t)$ in the form of equation (29) and C from equation (11),

$$\mathrm{i}\omega c l_g = (1+\mathrm{i})\frac{\chi\bar{C}D}{\mu_D\left(1-\bar{X}\right)}. \tag{31}$$

We now insert in equation (28) the equation (29) for $j_B(l_f, t)$ and the equation (31) for c, and we obtain the relation between the amplitude of the concentration wave and the periodic temperature T_{g_0} at the interface between the film and the gas, equation (19):

$$\chi\bar{C} = \varepsilon T_{g_0} \tag{32}$$

with

$$\varepsilon = \left\{(1-X)\frac{C_B}{T}\left(\frac{L}{RT}-1\right)\right\} \Big/ \left\{1 - X + (1-\mathrm{i})X\frac{\mu_D}{2l_g}\left[1 + \frac{l_g}{Y_P RTX}\right]\right\} \tag{33}$$

in which we assume $X \approx \bar{X} \gg |\chi|$, $T \approx \bar{T} \gg \left|\tilde{T}_g\right|$ and $C_B \approx \bar{C}_B = \bar{X}\bar{C} \gg |c_B|$.

Next we calculate the temperature amplitude T_{g_0} by applying the continuity of temperature and heat flux at the interfaces between the three media, equations (6) to (8). The heat generated by the absorption of light at the solid surface appears in the heat balance at the boundary $z = 0$:

$$Q_0\,\mathrm{e}^{\mathrm{i}\omega t} = k_s\left(\frac{\partial\tilde{T}_s}{\partial z}\right)_{z=0} - k_f\left(\frac{\partial\tilde{T}_f}{\partial z}\right)_{z=0} \tag{34}$$

and the heat associated with the adsorption/desorption process in the heat balance at the boundary $z = l_f$:

$$L\,j_B\left(l_f, t\right) = k_g\left(\frac{\partial\tilde{T}_g}{\partial z}\right)_{z=l_f} - k_f\left(\frac{\partial\tilde{T}_f}{\partial z}\right)_{z=l_f}. \tag{35}$$

The continuity of the temperature at the interfaces gives, at $z = 0$,

$$T_{s_0} = T_f^+ + T_f^- \tag{36}$$

and, at $z = l_f$,

$$T_{g_0} = T_f^+ d^+ + T_f^- d^- \tag{37}$$

where $d^{\pm} = \exp\left[\pm(1+\mathrm{i})\, l_f/\mu_f\right]$. By solving the system the four equations (34) to (37) we get an expression for the temperature amplitude at the film–gas interface, T_{g_0}:

$$T_{g_0} = \frac{(1-\mathrm{i})\, I_0}{b^+\left[\Lambda_s + \Lambda_g + \Lambda_D + (b^+/b^-)\Lambda_f\right] + b^-(\Lambda_s/\Lambda_g)\left(\Lambda_g + \Lambda_D\right) - 4\Lambda_f/b^-} \tag{38}$$

where $b^{\pm} = d^+ \pm d^-$, $\Lambda_i = k_i/\mu_i$ and $k_D = (LD\varepsilon)/(1-X)$.

The final expression of the mirage deflection is then deduced from relations (4), (6), (23), (32) and (33):

$$\Phi_n = -(1+\mathrm{i})\frac{1}{n}T_{g_0}\frac{RT_0}{P_0 T}\left\{\left[C_A\left(n_A^0 - 1\right) + C_B\left(n_B^0 - 1\right)\right]\frac{\mathrm{e}^{-(1+\mathrm{i})(z-l_f)/\mu_g}}{\mu_g}\right.$$
$$-C_B\left(n_B^0 - n_A^0\right)\frac{(1-X)\,(L/RT - 1)}{1 - X + (1-\mathrm{i})\,X(\mu_D/2l_g)\left[1 + l_g/Y_P RTX\right]}$$
$$\left.\times\frac{\mathrm{e}^{-(1+\mathrm{i})(z-l_f)/\mu_D}}{\mu_D}\right\} \tag{39}$$

where n and T_{g_0} are given by equations (2) and (38) respectively.

The first term in equation (39) represents the contribution of the thermal gradient and the second term the contribution of the concentration gradient. Notice that as long as we use air as a non-condensable gas, the two terms have opposite signs since for any condensable gas n_B^0 is larger than n_A^0. That means that, depending on experimental conditions, one or the other of the two terms can dominate or interferences may occur.

Expression (39) shows that the mirage deflection depends directly on adsorption through the isosteric heat of adsorption L and the slope of the adsorption isotherm $Y_P(P_B)$. Since we have verified experimentally that the mass diffusion contribution to the mirage signal dominates only when the vapour saturation conditions are approached (see part II of this work), we suppose that the adsorption process does not sensitively affect the mirage deflection unless multilayer adsorption takes place. In that case the adsorption heat L is well approximated by the vaporization heat L_0 and we can use L_0 instead of L in our calculations with equation (39). For the same reason we choose the BET equation, valid for multilayer adsorption [11], to calculate the function $Y_P(P_B)$. The BET equation is an adsorption isotherm that can be expressed as [12]

$$Y = Y_1\frac{c_1\, x}{(1-x)\,[1 + (c_1 - 1)\,x]} \tag{40}$$

where x is the relative pressure P_B/P_{sat}, P_{sat} the vapour saturation pressure, and Y_1 and c_1 are two parameters associated with the number of moles adsorbed on a monolayer and with the difference $L - L_0$, respectively. We have then

$$Y_P = \frac{\partial Y}{\partial P_B} = Y_1\frac{c_1\left[1 + (c_1 - 1)\,x^2\right]}{(1-x)^2\,[1 + (c_1 - 1)\,x]^2}\frac{1}{P_{sat}}. \tag{41}$$

Finally, to calculate the saturation pressure P_{sat} of gas B at temperature T we used the Antoine equation [12]

$$\ln(P_{sat}) = A_a - \frac{B_a}{T + C_a} \tag{42}$$

where A_a, B_a and C_a are constants for each substance, which can be found in physical data tables [12].

3. Analysis of the thermal contribution

Expression (39) is valid for the general case where mass diffusion due to periodic adsorption on the sample surface affects the mirage signal. When this mass contribution can be neglected, we obtain a much simpler relationship that can be derived from equation (39) by dropping the second term and making $l_f = 0$. This last condition also allows us to simplify the expression for T_{g_0}, the amplitude of the thermal wave at the gas/solid interface, which reduces to

$$T_{g_0} = \frac{(1-\mathrm{i})\, I_0}{2\left(\Lambda_s + \Lambda_g\right)} \cong (1-\mathrm{i})\,\frac{I_0}{2}\,\frac{\mu_s}{k_s} \tag{43}$$

since $\Lambda_s \gg \Lambda_g$, the indexes s and g referring to the solid and the gas mixture, respectively. The expression of the mirage deflection when the contribution of the concentration gradient can be neglected is then

$$\Phi_n \cong -\frac{I_0}{n}\,\frac{\sqrt{\alpha_s}}{k_s}\,\frac{1}{\sqrt{\alpha_g}}\,\frac{\bar{R}\,T_0}{P_0\,T}\left[C_A\left(n_A^0 - 1\right) + C_B\left(n_B^0 - 1\right)\right] \mathrm{e}^{-(1+\mathrm{i})z/\mu_g}. \tag{44}$$

3.1. The probe-beam/sample distance and modulation frequency

Equation (44) shows that the phase φ of the mirage deflection and the logarithm of the signal amplitude A are linear in both z, the probe-beam/sample distance, and $\sqrt{f}$, the square root of the modulation frequency. By measuring the amplitude and phase of the mirage deflection at different values of f or z we can get α_g, the thermal diffusivity of the gas mixture, from the slopes of $\ln A(\sqrt{f})$, $\varphi(\sqrt{f})$, $\ln A(z)$ or $\varphi(z)$. The linearity of these four functions can be used as a test to ensure that the experimental conditions satisfy the main assumptions that we made about the thermal contribution to the mirage signal: no three-dimensional (3D) effects, surface absorption of the pump beam, and no sample deformation.

For a few of the experimental conditions we used, the 3D effect of the probe-beam size could not be neglected. The expressions we obtained (equation (39) and (44)) give the mirage deflection of an elementary light ray (infinitely thin). The convolution with a gaussian function representing the spatial distribution of the laser beam energy takes into account the finite size of the probe beam. It can be shown [13] that, as a result of this convolution, each one of the terms containing the spatial dependency of the mirage deflection is multiplied by

$$\exp\left(\frac{\mathrm{i}\, r_s^2}{\mu_i^2}\right) \operatorname{erfc}\left[\frac{(1+\mathrm{i})\, r_s}{2\sqrt{2}\,\mu_i} - \frac{\sqrt{2}\, z}{r_s}\right] \tag{45}$$

where erfc is the complementary error function ($\operatorname{erfc}(x) = 1 - \operatorname{erf}(x)$; $i = \mathrm{g},\ \mathrm{c}$); μ_g is the gas thermal diffusion length; μ_D the mass diffusion length; r_s the probe-beam radius; and z the sample/probe-beam axis distance. This convolution effect can be expressed simply as $\exp(\mathrm{i}r_s^2/\mu_i^2)$ when $r_s/\mu_i < 2\sqrt{2}$, as is the case in all of our experiments. In fact, for most of them the condition $r_s/\mu_t \ll 1$ holds and the probe-beam convolution effect can be neglected. When this is not the case the function $\varphi(\sqrt{f})$ is no longer linear if we do not probe at a distance z that is much larger than the probe-beam radius r_s.

3.2. Temperature and total pressure

By writing the gas thermal diffusion length as

$$\mu_g = \sqrt{\frac{\alpha_g}{\pi f}} = \sqrt{\frac{k_g}{\pi f \rho_g c_{pg}}} = \sqrt{\frac{k_g R}{\pi f M_g c_{pg}}} \sqrt{\frac{T}{P}} \tag{46}$$

and $C_i = P_i/RT$, $i = \mathrm{A}, \mathrm{B}$, we find the mirage deflection in the absence of adsorption to be

$$\Phi_n \propto P^{3/2} T^{-5/2} \mathrm{e}^{-(1+\mathrm{i})\delta\sqrt{P/T}} \tag{47}$$

where

$$\delta = z \sqrt{\frac{\pi f M_g c_{pg}}{k_g R}}. \tag{48}$$

Equation (47) shows that the phase of the mirage deflection decreases when the total pressure P increases or the temperature decreases. The amplitude of the mirage signal will increase or decrease when P (or T) increases depending on the values of δ, P and T. For the experimental conditions we used, with T and P close to the normal temperature and pressure, the amplitude A increases when T decreases and, for the lowest values of the total pressure P, it increases with P. If δ is high enough (high values of z and f) the amplitude may decrease slightly when P increases above a certain value that depends on the actual value of δ (see figure 2).

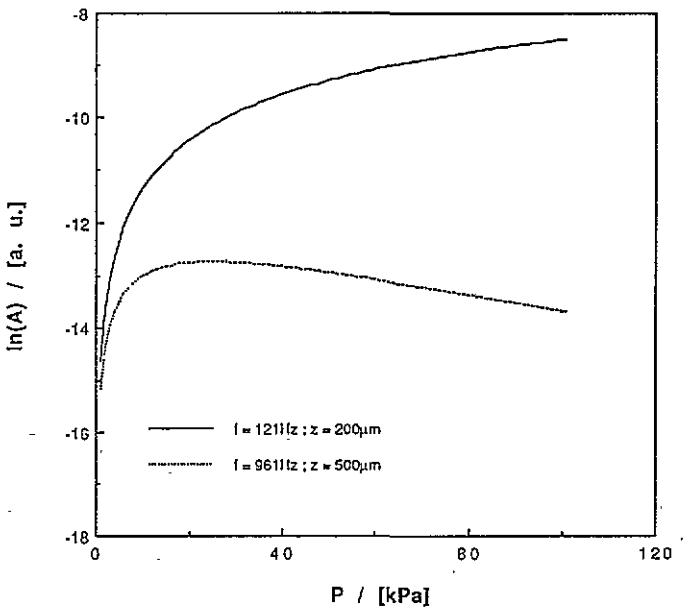

Figure 2. Calculated curves for $\ln A(P)$ when the thermal contribution dominates (equation (44)). The amplitude A of the mirage signal increases with P for most of our experimental conditions, except when we use simultaneously a high modulation frequency f and a large sample/probe-beam distance z (dotted line).

We must keep in mind that the thermal conductivity of the gas mixture k_g, and the thermal properties of the sample (α_s, k_s) are temperature dependent too. However, if the temperature is kept always close to the ambient temperature, α_s and k_s are approximately

constant and k_g will increase monotonically with T [12] thus not affecting the above conclusions about the dependence of $\Phi_n(T)$.

Knowing how the thermal contribution of the mirage deflection varies with the temperature T and the total pressure P, we can more easily detect any contribution due to mass diffusion.

3.3. The composition of the gas mixture

To evaluate the effect of changing the molar fraction X of the adsorbable vapour it would be necessary to specify the components of the gas mixture. We can note that the molar fraction X affects the thermal contribution of the mirage deflection (equation (44)) through C_A and C_B (equation (10)), n (equation (2)), α_g and μ_g (equation (9)).

The thermal diffusivity of the gas mixture α_g is given by $\alpha_g = k_g/(\rho_g c_{pg})$ where the thermal conductivity k_g, the density ρ_g and the isobaric specific heat capacity c_{pg} of the mixture were calculated using the following equations:

$$k_g = \frac{1}{2}\left[(1-X)\,k_A + Xk_B + \frac{1}{(1-X)/k_A + X/k_B}\right] \tag{49}$$

$$\rho_g = [(1-X)\,\rho_A + X\rho_B] \tag{50}$$

$$c_{pg} = (1-X)\,c_{pA} + Xc_{pB}. \tag{51}$$

Since these expressions are approximate, introducing an error that is difficult to estimate, experimental determination of α_g from the slopes of $\ln A(z)$, $\varphi(z)$, $\ln A(\sqrt{f})$ and $\varphi(\sqrt{f})$ can be very useful for validating the value of α_g.

4. Analysis of a dominant mass diffusion contribution

When the first term in equation (39) can be neglected as compared with the last term, the general expression for the mirage deflection can be reduced to

$$\Phi_n \cong (1+\mathrm{i})\,\frac{\mathrm{i}}{n} T_{g_0} \varepsilon \frac{R\,T_0}{P_0\,T}\left(n_B^0 - n_A^0\right)\frac{\mathrm{e}^{-(1+\mathrm{i})(z-l_f)/\mu_D}}{\mu_D} \tag{52}$$

where n, T_{g_0} and ε are given by equations (2), (38) and (33) respectively.

If the mass diffusion contribution dominates then, as equation (52) clearly shows, φ and $\ln A$ are once again linear functions of z, the sample/probe-beam distance. The slopes of $\ln A(z)$ and $\varphi(z)$ give in this case the mass diffusion length $\mu_D = \sqrt{(D/\pi f)}$ allowing for an experimental determination of the diffusion coefficient D of the binary mixture. This could be a new interesting application of the mirage method since there are very few data on diffusion coefficients of gas mixtures.

From equation (52) we learn also that φ and $\ln A$ are not linear functions of $\sqrt{f}$ as they were for the thermal contribution. Indeed the modulation frequency appears not only in the exponential factor but also in T_{g_0}, ε and μ_D^{-1}. However, for the range of experimental values of f that we used, $\ln A(\sqrt{f})$ and $\varphi(\sqrt{f})$ are almost linear when the mass diffusion contribution dominates (see section 5.2).

5. Simulation of the mirage deflection

To study the effect of mass diffusion on the mirage deflection we calculate the amplitude and phase of the signal using equation (39). We choose a specific solid–gas system and a

given set of values of the experimental parameters and then we calculate curves for $\ln A$ and φ as functions of each one of the parameters.

The results that we present in this section were obtained for a stainless steel sample and a mixture of methylene chloride (CH_2Cl_2), as the adsorbable vapour, and argon. The data concerning the physical properties of these materials are taken from the literature [12, 14, 15]. The initial values of the experimental parameters in these calculations are: sample/probe-beam distance $z = 200$ μm; modulation frequency $f = 121$ Hz; total pressure $P = 50$ kPa; temperature $T = 294$ K; molar fraction of the adsorbable vapour (CH_2Cl_2) $X = 0.94$. These conditions have been chosen because they correspond to the experimental observation of a large mass diffusion contribution in mirage experiments.

We are especially interested in the transition where the thermal and the mass diffusion have the same order of magnitude. We establish that the most direct way of producing such a transition is by varying $Y_P(P_B)$, the slope of the adsorption isotherm. The experimental parameters that affect $Y_P(P_B)$ are the temperature T that defines the saturation pressure P_{sat}, and the partial pressure of the adsorbable vapour P_B which will be changed in two ways, either by varying the total pressure P and keeping the mole fraction X constant, or by varying X and keeping P constant. Both T and P affect the partial pressure $x = P_B/P_{sat}$ strongly, producing important changes in $Y_P(P_B)$ when x approaches unity.

The value of $Y_P(P_B)$ is directly proportional to Y_1, a parameter of the BET equation (40) related to the number of moles adsorbed on a monolayer. For this reason all our curves are calculated for three different values of Y_1: a very low value (10^{-8} mol m^{-2}) corresponding to a negligible mass diffusion contribution; a very high value (10^{-2} mol m^{-2}) producing a dominant mass diffusion effect; and an intermediate value (10^{-5} mol m^{-2}) which allows us to see the transition between the two domains when a specific parameter is changed.

In all the results presented here the parameter c_1 in equation (40) is kept constant, $c_1 = 1$, and the value used for the adsorbed film thickness ($l_f = 10^{-8}$ m) is small enough not to affect the results (see section 5.5).

5.1. The sample/probe-beam distance

Figure 3 presents the calculated curves for $\ln A(z)$ and $\varphi(z)$. We find as expected that these functions are linear when one or the other of the contributions dominates. In the intermediate case (10^{-5} mol m^{-2}) they are almost linear too because the values of the thermal (μ_g) and the mass (μ_c) diffusion lengths for this gas mixture are very similar. Notice also that when passing from a thermal to a mass diffusion effect the amplitude of the mirage deflection increases, particularly for the larger values of z, and the phase decreases, by almost 180° for very small distances z but by only 50° within 1 mm of the surface.

5.2. The modulation frequency

The results of the calculations for $\ln A(\sqrt{f})$ and $\varphi(\sqrt{f})$ are presented in figure 4. We see that for 1 Hz $< f <$ 1 kHz these functions are linear (or almost linear) when the thermal (mass diffusion) term dominates. When both effects contribute significantly to the mirage deflection, an increase of the modulation frequency can produce a transition from a thermal effect (at low frequencies) to a mass diffusion effect (at the higher frequencies). This transition can be identified in figure 4 by the phase shift of almost 180° associated with a rapid decrease of the amplitude, due to partly destructive interference between the thermal and the mass diffusion effects.

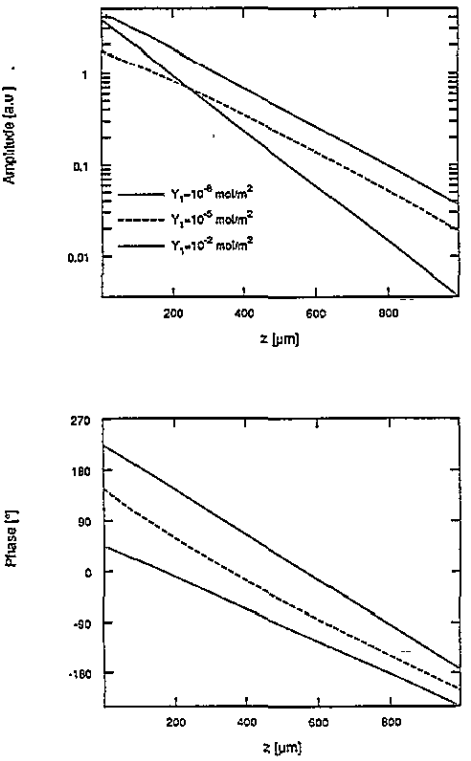

Figure 3. The dependence of the amplitude and the phase of the mirage deflection on the sample/probe-beam distance z. The curves were obtained from calculations for a mixture of CH_2Cl_2 with argon ($X = 0.94$), at $P = 50$ kPa, $f = 121$ Hz, $T = 294$ K, made with equation (39) in which $c_1 = 1$, $l_f = 0.1$ μm and for three values of Y_1.

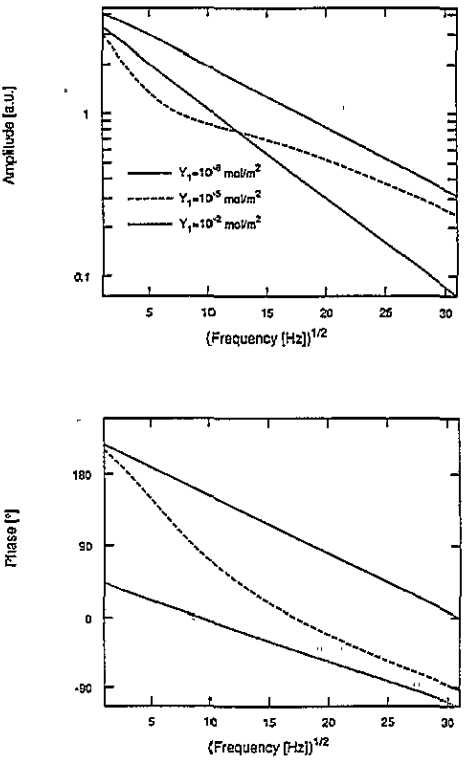

Figure 4. The dependence of the amplitude and the phase of the mirage deflection on the square root of the modulation frequency $\sqrt{f}$, for the same gas mixture as in figure 3. The curves were obtained from calculations made with equation (39) for $z = 200$ μm, $p = 50$ kPa, $T = 294$ K and three values of Y_1.

5.3. The total pressure

We show in figure 5 the curves for $\ln A(P)$ and $\varphi(P)$ for the same three values of Y_1 as in the previous figures. For $Y_1 = 10^{-8}$ mol m^{-2} the thermal effect dominates over the whole range of P-values, from the lowest pressures to the saturation of the CH_2Cl_2 vapour (corresponding to the upper limit of the x-axis). The curves for $Y_1 = 10^{-2}$ mol m^{-2} indicate that the mass diffusion contribution becomes dominant only at the higher pressures (corresponding to $P_B \geqslant P_{sat}/2$) while at lower pressures there is a transition from a thermal to a mass diffusion effect as P increases. With $Y_1 = 10^{-5}$ mol m^{-2} we see that this same transition, characterized by a phase shift of almost 180° and a minimum of the amplitude, takes place at much higher pressures very close to the vapour saturation pressure.

To demonstrate the sensitivity of the mirage deflection to the parameter Y_1 when the total pressure is varied, we present in figure 6 another set of curves for $\ln A(P)$ and $\varphi(P)$ for values of Y_1 ranging from 10^{-6} mol m^{-2} to 10^{-3} mol m^{-2}.

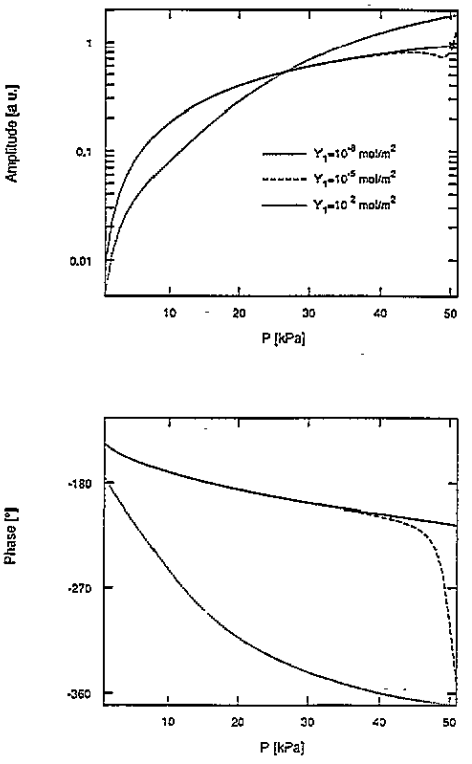

Figure 5. The dependence of the amplitude and the phase of the mirage deflection on the total pressure P, for the same gas mixture as in figure 3. The curves were obtained from calculations made with equation (39) for $z = 200$ μm, $f = 121$ Hz, $T = 294$ K and three values of Y_1.

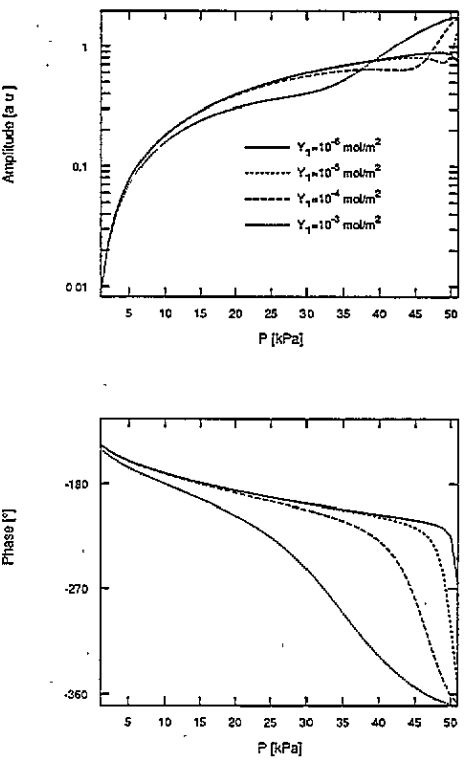

Figure 6. Calculated curves for $\ln A(P)$ and $\varphi(P)$ for different values of Y_1 showing the great sensitivity of the mirage signal to this parameter, for the same gas mixture as in figure 3. $z = 200$ μm, $f = 121$ Hz, $T = 294$ K.

5.4. The temperature

In figure 7 we present the calculated curves for $\ln A(T)$ and $\varphi(T)$. These curves show that over the whole range of T-values the thermal effect dominates when $Y_1 = 10^{-8}$ mol m^{-2} and the mass diffusion contribution dominates when $Y_1 = 10^{-2}$ mol m^{-2}. For $Y_1 = 10^{-5}$ mol m^{-2} we see the transition from a thermally dominated effect at the higher temperature to an effect essentially dominated by the mass diffusion contribution when the temperature T is reduced and, in this way, the saturation conditions are approached. As was mentioned before, this transition is characterized by a phase shift of almost 180° accompanied by a minimum of the amplitude of the mirage deflection. We wish to point out that a variation of less than 3 °C can produce an almost complete transition between the thermal and the mass diffusion domains.

5.5. Other parameters

In order to obtain a transition between the thermal and the mass diffusion domains we can also vary the mole fraction of the adsorbable vapour X but, since experimentally we also change the total pressure P when we vary X, the calculation of $\ln A(X)$ and $\varphi(X)$ has no

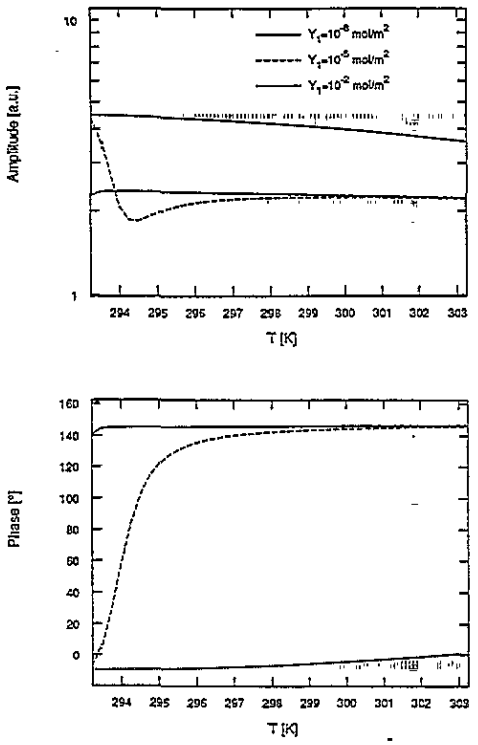

Figure 7. The dependence of the amplitude and the phase of the mirage deflection on the temperature T, for the same gas mixture as in figure 3. The curves were obtained from calculations made with equation (39) for three values of Y_1. $z = 200$ μm, $f = 121$ Hz, $P = 50$ kPa.

practical use. Notice, however, that if we hold P constant a small change in X can strongly affect the mirage signal through $x = P_B/P_{sat} = XP/P_{sat}$.

All the curves presented here were calculated using the value $c_1 = 1$ for the second parameter in the BET adsorption isotherm (equation (40)). We verified that we can vary the value of c_1 between 10^{-2} and 10^3 without producing any effect on the calculated curves as long as we keep the product $c_1 Y_1$ constant (see equations (40) and (41)). Since c_1 gives the influence of the first monolayer on the shape of the adsorption isotherm [11], our results seem to indicate that for our experimental conditions there is no sensitivity to the adsorption of the first monolayer. This can be easily explained: the minimum number of vapour molecules to be adsorbed and desorbed during each cycle for the mass diffusion contribution to be at least as large as the thermal contribution can only be attained with multilayer adsorption.

6. Conclusions

We developed a theoretical model for the mirage deflection valid when the mass diffusion contribution due to the induced periodic adsorption/desorption of vapour molecules at the solid sample surface becomes non-negligible and we discussed the limits of validity of this very simple one-dimensional model which is useful when physical adsorption occurs on a non-porous sample in conditions close to the normal temperature and pressure.

To study the influence of the experimental parameters and the sensitivity of the mirage signal to the adsorption process we used the expression we derived for Φ_n, the mirage deflection, to calculate curves for the amplitude and phase of Φ_n as functions of each one of the parameters. We found that the phase of the mirage signal is remarkably sensitive to

the number of molecules in one adsorbed monolayer (Y_1) when a transition occurs between a thermally dominated effect and a mass-diffusion-dominated effect. Usually, for this transition to take place the saturation conditions of the vapour must be approached and the mirage signal appears to be insensitive to the first adsorbed monolayer.

There are several experimental parameters that can be varied in order to produce the transition between a thermally dominated effect and a mass-diffusion-dominant contribution, thus allowing the study of the adsorption process with maximal sensitivity. We found, however, that by varying the temperature T or the total pressure P (while the gas composition was kept constant) we obtained a faster and more complete transition since these two parameters strongly affect the magnitude of the mass diffusion contribution.

As a result of our study we found that the mirage method can be used to measure experimentally the thermal diffusivity and the mass diffusion coefficient of gas mixtures. There are currently very few data available on these diffusion properties and this should become a new important application of the mirage deflection technique.

References

[1] Somasundaram T and Ganguly P 1983 *J. Physique Coll.* **44** C6 239
Srinivasan J, Kumar R and Gandhi K S 1987 *Appl. Phys.* B **43** 35
[2] Korpiun P 1984 *Appl. Phys. Lett.* **44** 675
[3] Korpiun P, Herrmann W, Kindermann A, Rothmeyer M and Büchner B 1986 *Can. J. Phys.* **64** 1064
[4] Lepoutre F, Rousset G, Plichon V and Rollat N 1988 *Photoacoustic and Photothermal Phenomena* ed P Hess and J Pelzl (Berlin: Springer) p 187
[5] Korpiun P, Osiander R, Schmitt H and Micheler W 1991 *Appl. Phys.* A **52** 223
[6] Silva M Z, Forge P, Lepoutre F and Korpiun P 1992 *Photoacoustic and Photothermal Phenomena III* ed D Bicanic (Berlin: Springer) p 651
[7] Born M and Wolf E 1991 *Principles of Optics* 6th edn (Oxford: Pergamon) section 2.3, p 84
[8] Lepoutre F 1983 *J. Physique Coll.* **44** C6 3
[9] Bird R B, Stewart W E and Lightfoot E N 1960 *Transport Phenomena* (New York: Wiley) p 502
[10] Young D M and Crowell A D 1962 *Physical Adsorption of Gases* (London: Butterworths) pp 3, 152
[11] Adamson A W 1982 *Physical Chemistry of Surfaces* (New York: Wiley) pp 517, 537, 570
[12] Reid R C, Prausnitz J M and Sherwood T K 1977 *The Properties of Gases and Liquids* (New York: McGraw-Hill)
[13] Legal-Lasalle E, Lepoutre F and Roger J P 1988 *J. Appl. Phys.* **64** 1
[14] *Landolt–Börnstein New Series: Zahlenwerte und Funktionen aus Physik, Chemie, Astronomie, Geophysik, Technik* 1961 vol 2, parts 4, 5a and 8; vol 4, parts 4a and 4b (Berlin: Springer)
[15] Touloukian Y S and Ho C Y 1976 *Thermophysical Properties of Matter* vols 3, 6 (New York: Plenum)